

Spatially resolved photoluminescence in GaAs surface acoustic wave structures

P. V. Santos,^{a)} M. Ramsteiner, and F. Jungnickel

Paul-Drude-Institut für Festkörperelektronik, Hausvogteiplatz 5-7, D-10117 Berlin, Germany

(Received 23 December 1997; accepted for publication 27 February 1998)

The interaction between a surface acoustic wave (SAW) and the excitonic photoluminescence (PL) in GaAs SAW structures is investigated. The dependence of the PL on the SAW amplitude and illumination intensity is explained by a simple model based on the field-induced ionization of the excitons and on the screening of the SAW electric field by photogenerated carriers. Microscopic PL constitutes a powerful technique for spatially resolving electric-field distributions in SAW structures. © 1998 American Institute of Physics. [S0003-6951(98)02517-0]

Surface acoustic waves (SAW's) interact strongly with photogenerated carriers in piezoelectric semiconductors. The strain and the piezoelectric fields accompanying the SAW modify energy levels and wave functions in the semiconductor, and thus their optical properties. In particular, the SAW electric field is very effective in modulating the excitonic absorption in semiconductors: this mechanism has been proposed as the operation basis of electro-optical modulators¹ and optical memories² of GaAs-based structures.

The effects of a continuous electric field on the excitonic transitions are well documented in the literature.^{3,4} In this letter, we will demonstrate that the spatially varying character of the SAW electric field leads to new effects in the excitonic photoluminescence (PL). In particular, the PL intensity becomes strongly dependent on the excitation amplitude due to the screening of the SAW electric field by photogenerated carriers. We further show that microscopic (μ -) PL measurements constitute a powerful tool for the contactless mapping of electric fields in SAW structures with lateral resolution comparable to that achieved by optical probes of the acoustic displacement field.^{5,6}

The experiments reported here were performed on SAW-delay lines fabricated on (100) undoped GaAs substrates (see Fig. 1) with the SAW propagating along the [011] direction. The split-finger interdigital transducers (IDT's) were designed for operation at a SAW wavelength $\lambda_{\text{SAW}}=14.4 \mu\text{m}$, corresponding to a frequency of 199.4 MHz at 10 K. The transducers, with an aperture of $330 \mu\text{m}$, consist of 700 pairs of 60 nm thick and $1.8 \mu\text{m}$ wide gold electrodes, with the centers spaced by $3.6 \mu\text{m}$. For the μ -PL measurements the samples were mounted in a liquid-helium cryostat ($T\sim 8-10 \text{ K}$) with radio-frequency (RF) feedthroughs. The exciting light, either from an Ar^+ ($\lambda_L=514.5 \text{ nm}$) or from a Kr^+ ($\lambda_L=676.4 \text{ nm}$) laser, was focused down to a spot diameter $\phi_L\sim 3 \mu\text{m}$ on the sample surface using a $50\times$ (numerical aperture 0.55) microscope objective. The PL light was collected by the same objective and analyzed by a DILOR triple spectrograph equipped with a cooled charge-coupled-device detector array. The

micro-PL profiles were obtained by scanning the laser spot on the sample surface.

The PL spectrum in the absence of RF power applied to the IDT (upper curve in Fig. 1) is dominated by the emission lines from free and bound excitons. The transition assignments in the Fig. 1 are based on Ref. 7. The dominant features correspond to emission from the free exciton (FE, 1.515 eV), from the neutral acceptor-bound exciton (AX, 1.5123 eV), and from the carbon-bound exciton (C, 1.494 eV). When a SAW is launched from one of the transducers (lower curve), the PL lines decrease in intensity and broaden. These effects are attributed to the ionization of the excitons by the electric-field \mathcal{E}_{SAW} accompanying the SAW.^{2-4,8} This field is elliptically polarized in the SAW sagittal plane with components \mathcal{E}_x and \mathcal{E}_z along the $x=[011]$ and $z=[100]$ directions, respectively, dephased by 90° . The FE PL probes this field within a $1/\alpha\sim 1 \mu\text{m}$ thick surface layer, where α is the absorption coefficient at the emission wavelength.

The field interacts with the exciton through different mechanisms. At low fields ($<1 \text{ kV/cm}$), the exciton line

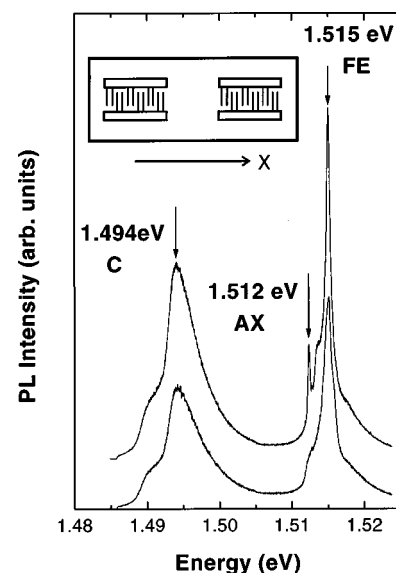


FIG. 1. GaAs photoluminescence without (upper curve) and under the influence of a surface acoustic wave (lower curve), recorded with an excitation wavelength $\lambda_L=514.5 \text{ nm}$. The spectra are displaced vertically. The inset shows the configuration of the transducers.

^{a)}Electronic mail: santos@pdi-berlin.de

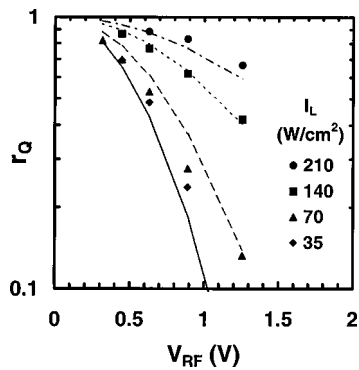


FIG. 2. Dependence of the luminescence quenching r_Q on the RF voltage V_{RF} and on the excitation intensity I_L (symbols).

redshifts and broadens through the quadratic Stark effect; for higher fields, field-induced ionization sets in.^{3,4} Exciton ionization can also be induced by impact with carriers: this mechanism has been proposed as the main source of PL quenching and broadening under homogeneous fields.³ Although the details of the impact ionization process is certainly different under the inhomogeneous SAW field, the strong PL quenching is probably also due to the same mechanism. The propagating field separates the photogenerated electron and holes and sweeps them out of the measurement spot (of diameter $\phi_L \sim 3 \mu\text{m} < \lambda_{\text{SAW}}$), thus further reducing the recombination probability.² Finally, the electric field also modulates the optical response in the continuum range of the electron-hole transitions (Franz-Keldysh effect^{4,9}). The last mechanism is responsible for an apparent blueshift of the PL line (not resolved in the scale of Fig. 1). The maximum shift (up to 0.22 meV for the highest applied RF power of $\sim 1.25V_{\text{rms}}$) corresponds to that measured under a dc field of $\sim 5.5 \text{ kV/cm}$.⁴

The PL quenching, defined as the ratio r_Q between the PL with and without the SAW, is plotted in Fig. 2 as a function of the RF voltage V_{RF} applied to the IDT for different illumination intensities I_L . The RF voltage necessary to achieve a certain r_Q increases with illumination intensity: the effect is attributed to a partial compensation (screening) of the piezoelectric field by photogenerated carriers trapped in the positive and negative potential wells created by the field. We present in the following a simple phenomenological model for the PL quenching based on a reduction of the effective exciton binding-energy $E_{\text{ex}}(\mathcal{E})$ in the presence of an electric field (\mathcal{E}). Specifically, we will assume that $E_{\text{ex}}(\mathcal{E}) = E_{\text{ex}}(0) - E_k$, with E_k proportional to \mathcal{E}^2 , i.e., $E_k = c_1 \mathcal{E}^2$ ($c_1 \equiv \text{constant}$). For the impact ionization mechanism, the energy reduction E_k may be related to the kinetic energy gained by the photogenerated carriers in the electric field, i.e., $E_k \sim \frac{1}{2} m^* (\mu \mathcal{E})^2$. Here, μ and m^* are the carrier mobility and effective mass, respectively. The exciton lifetime $\tau(\mathcal{E})$ (relative to dissociation in electrons and holes) thus becomes: $\tau(\mathcal{E}) = \tau_0 e^{-c_1 \cdot \mathcal{E}^2 / kT}$, where τ_0 is the corresponding lifetime in the absence of the field. The PL quenching r_Q is then related to \mathcal{E} by the following expression:

$$r_Q = \frac{\tau(\mathcal{E})}{\tau_0} = e^{-c_1 \mathcal{E}^2 / kT}. \quad (1)$$

In a SAW, the field \mathcal{E} in Eq. (1) includes the effects of

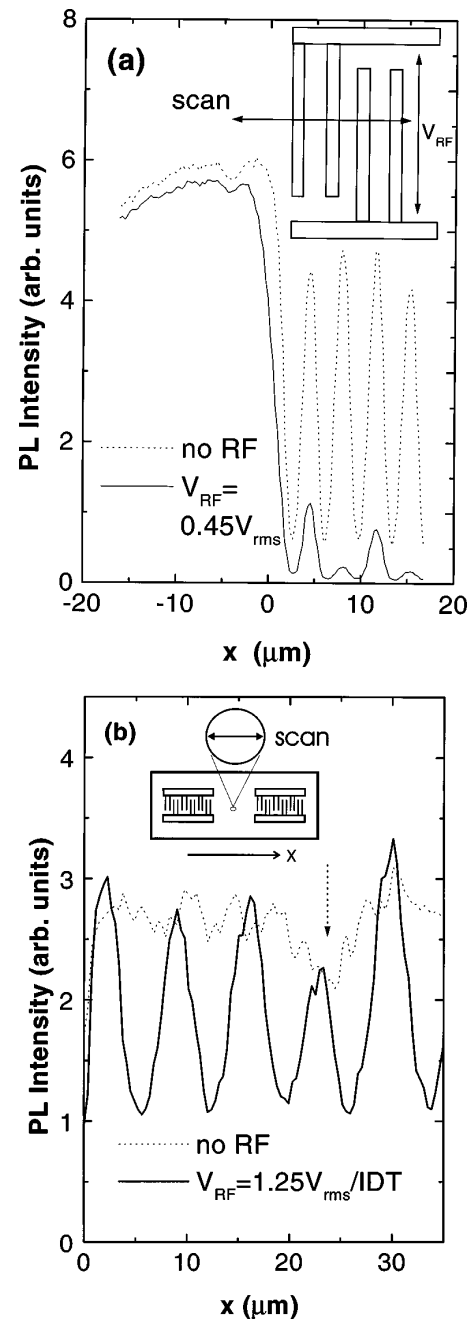


FIG. 3. (a) Free-exciton luminescence profiles (emission at 1.515 eV) close to the edge of the IDT and (b) under a standing wave between the IDT's. The solid and dashed lines display the corresponding profiles for powered and unpowered IDT's, respectively. The insets show the corresponding scan regions.

both the piezoelectric SAW field \mathcal{E}_{SAW} (proportional to V_{RF}) and of its screening by a density n_s of photogenerated carriers separated by the field. Assuming the rate $\partial n_s / \partial t \sim \mathcal{E} I_L$, one obtains under steady-state conditions the following first-order approximation for \mathcal{E} :

$$\mathcal{E} = \frac{1}{1 + c_2 I_L} \mathcal{E}_{\text{SAW}}, \quad (2)$$

where c_2 is a proportionality factor. The lines in Fig. 2 were obtained by fitting the constants c_1 and c_2 in the expression of r_Q [Eqs. (1) and (2)] to the whole set of experi-

mental data. A reasonable agreement is obtained with the experimental data, indicating that the model describes the physical situation.

The strong field dependence makes the μ -PL a sensitive probe for the electric-field distribution in SAW structures. Two examples are given in Fig. 3. The dashed line in Fig. 3(a) shows the spatial dependence of the FE luminescence (integrated within a 10 meV region around the FE line) obtained while scanning the laser beam close to the edge of an unpowered IDT (see the inset). The metal electrodes appear as minima spaced by $\lambda_{\text{SAW}}/4$: the sinuslike line shape arises from the finite lateral spatial resolution. The solid line reproduces the same profile when a RF voltage of 0.4 V is applied to the IDT. The slight PL quenching away from the IDT is caused by the electric field associated with the SAW launched by the transducer. In the electrode region, the SAW field is superimposed on the much stronger electric field generated by the applied RF voltage. The latter is oriented along the x direction close to the surface and vanishes between the split fingers. As a consequence, the PL oscillations display a periodicity of $\lambda_{\text{SAW}}/2$.

The field distribution between the transducers can be accessed if a standing wave is created by interfering SAW's launched simultaneously from two IDT's, as illustrated in the inset of Fig. 3(b). The dashed line in Fig. 3(b) shows the free-exciton PL profile recorded between the IDT's (see the inset in Fig. 1) with unpowered transducers. The PL displays fluctuations (such as those indicated by the dashed arrow) attributed to defects and inhomogeneities on the sample surface. The solid line in Fig. 3(b) reproduces the same profile in the presence of a SAW standing wave. The PL profile exhibits oscillations with a periodicity of $\lambda_{\text{SAW}}/2$, thus evidencing the presence of a spatially static electric-field distribution. Note that the variation in the amplitude of the FE oscillation maxima closely follows the inhomogeneities in the surface response (see the dotted line). The minima, however, are less position dependent.

Due to the elliptical polarization of the SAW field, the nodes of \mathcal{E}_z and \mathcal{E}_x in a standing-wave field are displaced by $\lambda_{\text{SAW}}/4$: as a result, the spatial modulation of the field depends on the relative amplitudes of \mathcal{E}_z and \mathcal{E}_x . The maxima

of the FE PL under a standing wave correspond closely to the PL without applied field, thus suggesting that one of the field directions is much less effective in quenching the PL than the other. Note, however, that the model presented above for the PL quenching induced by a propagating SAW cannot be directly applied to the present situation: this model neglects the dynamics of the carriers in the field and can, thus, not account for the recombination that takes place when the standing-wave field vanishes twice in an oscillation cycle. Investigation of the carrier dynamics under these conditions and including the effects of surface states are currently underway.

In conclusion, the interplay between photogenerated carriers, excitons, and the piezoelectric fields leads to a strong dependence of the PL from GaAs SAW structures on both the SAW amplitude and the excitation intensity. The high PL sensitivity to electric fields makes the μ -PL a powerful tool for the contactless sampling of the field distribution in SAW semiconductor structures. Though restricted to low temperatures in GaAs, the technique becomes operational at room temperatures in materials with high exciton binding energies¹⁰ such as quantum-well structures and II–VI compounds.

The authors thank T. Hesjedal, H. Grahn, E. Chilla, and H. J. Fröhlich for helpful discussions, and R. Nötzel for a critical reading of the manuscript. The authors acknowledge the expertise of W. Seidel and K. Hauck in the fabrication of the SAW structures.

¹F. Jain and K. Bhattacharjee, Proc. SPIE **1347**, 614 (1990).

²C. Rocke, S. Zimmermann, A. Wixforth, J. P. Kotthaus, G. Böhm, and G. Weimann, Phys. Rev. Lett. **78**, 4099 (1997).

³W. Bludau and E. Wagner, Phys. Rev. B **13**, 5410 (1976).

⁴L. Schultheis, K. Köhler, and W. Tu, Phys. Rev. B **36**, 6609 (1987).

⁵A. Holm, W. Ruile, and R. Weigel, Int. J. Electron. Commun. **2**, 91 (1997).

⁶S. Jen and C. Hartmann, 1996 IEEE Ultras. Symp. Proc., 33 (1996).

⁷L. Pavesi and M. Guzzi, J. Appl. Phys. **75**, 4779 (1994).

⁸M. A. Jakobson, V. D. Kagan, R. Katilius, and G. O. Müller, Sov. Phys. Solid State **161**, 595 (1990).

⁹D. A. Aspnes and A. A. Studna, Phys. Rev. B **7**, 4605 (1973).

¹⁰M. Rotter, C. Rocke, G. Böhm, A. Lorke, A. Wixforth, W. Ruile, and L. Korte, Appl. Phys. Lett. **70**, 2097 (1997).